IEEE Access
Multidisciplinary | Rapid Review | Open Access Journal

Received 31 October 2023, accepted 26 November 2023, date of publication 30 November 2023,
date of current version 6 December 2023.

Digital Object Identifier 10.1109/ACCESS.2023.3338135

RESEARCH ARTICLE

A Compact Filtering Antenna With Step and Continuous Tuning Modes for WiMAX Cognitive Radio Communication

FALIH M. ALNAHWI[1], ABDULGHAFOR A. ABDULHAMEED[2,3], NAZAR T. ALI[4], (Senior Member, IEEE), YASIR I. A. AL-YASIR[5],(Member, IEEE), ZDENĚK KUBÍK[2], ABDULKAREEM S. ABDULLAH[1], (Senior Member, IEEE), AND RAED A. ABD-ALHAMEED[5,6], (Senior Member, IEEE)

[1]Department of Electrical Engineering, College of Engineering, University of Basrah, Basrah 61001, Iraq
[2]Department of Electronics and Information Technology, Faculty of Electrical Engineering, University of West Bohemia, 301 00 Pilsen, Czech Republic
[3]Department of Electrical Techniques, Qurna Technique Institute, Southern Technical University, Basrah 61001, Iraq
[4]Department of Electrical Engineering and Computer Science, Khalifa University, Abu Dhabi, United Arab Emirates
[5]Bradford-Renduchintala Centre for Space AI, Faculty of Engineering and Informatics, University of Bradford, BD7 1DP Bradford, U.K.
[6]Department of Information and Communication Engineering, Basrah University College of Science and Technology, Basrah 61004, Iraq

Corresponding author: Raed A. Abd-Alhameed (r.a.a.abd@bradford.ac.uk)

This work was supported in part by the Innovation Programme under Grant H2020-MSCA-ITN-2016 SECRET-722424, and in part by the U.K. Engineering and Physical Sciences Research Council (EPSRC) under Grant EP/E022936/1.

ABSTRACT This work presents a combination of a cup-shaped monopole antenna and an E-shaped Multi-Mode Resonator (MMR) with the presence of a pair of PIN diodes and a varactor diode to form a compact reconfigurable communication filtering antenna for interweave Cognitive Radio (CR) systems. The proposed filtering antenna operates in the WiMAX band, and it is fabricated on an FR4 substrate with overall dimensions normalized to the wavelength (λ_o) of the first resonant frequency ($0.413\lambda_o \times 0.516\lambda_o \times 0.0165\lambda_o$). The step and continuous tuning serve the secondary user of the WiMAX CR system to communicate in the absence of the primary users at modifiable resonant frequencies and data rates.When the PIN diodes are OFF, the filtering antenna operates with a fixed odd mode resonant frequency and tunable even mode resonant frequency. This state results in a tunable antenna bandwidth covering a maximum measured frequency range of $3.25-4.02$ *GHz* and a minimum measured range equal to $3.25-3.58$ *GHz*. The ON state of the PIN diodes eliminates the antenna matching at the even mode resonant frequency while keeping a strong matching at the odd mode resonant frequency. The resulted operational measured frequency range of the antenna in this state is fixed at $2.9-3.28$ *GHz*. The filtering antenna has acceptable gain values at the pass band of the E-shaped MMR with a maximum simulated gain value equal to 2.5 *dB* and a measured maximum gain equal to 2.48 *dB*. The simulated and measured power patterns of the antenna for all diodes states are omnidirectional, which are convenient for portable CR gadgets.

INDEX TERMS Cognitive radio, even and odd mode analysis, filtering antenna, multi-mode resonator, reconfigurable antenna.

I. INTRODUCTION

The congestion of the allocated spectrum has fueled the researchers to develop a new approach that utilizes the unused spectrum for the communication of another user. Cognitive Radio (CR) has emerged as a new technology that meets the aforementioned requirements. Since 70% of the allocated spectrum is idle for a noticeable amount of time [1], CR specifies the spectrum of the idle ''primary user'' for another active user called the ''secondary user''. This

The associate editor coordinating the review of this manuscript and approving it for publication was Yuh-Shyan Hwang.

© 2023 The Authors. This work is licensed under a Creative Commons Attribution-NonCommercial-NoDerivatives 4.0 License.
For more information, see https://creativecommons.org/licenses/by-nc-nd/4.0/

technology requires a sensing system that explores the status of the channel and a communication system for information exchange. The communication system of the CR needs a frequency reconfigurable antenna to avoid interference with the primary user during his active mode. When PIN diodes or MEMS switches are used, a step tuning is obtained in the communication antenna. On the other hand, the continuous tuning of the communication antenna is attained when the varactor diode is used to tune its frequency domain characteristics. Unfortunately, the radiation pattern of the conventional CR communication antennas is heavily distorted because the switching elements and their biasing lines are located on the antenna radiating patch [2], [3]. Therefore, reconfigurable filtering antennas are preferable in these kinds of applications as long as the switching elements are mounted on the filter part instead of the antenna radiating patch.

Many reconfigurable filtering antennas were proposed to manipulate the communication mode of the CR systems. A band-pass filter was inserted in the feeding line of a Vivaldi antenna with a varactor diode to form a filtering antenna with continuous tuning along the range (6.2-6.5 GHz) [4], [5]. A miniaturized capacitively loaded loop resonator was attached to a monopole antenna to restrict the radiation of the antenna within the unlicensed industrial-scientific-medical band [6]. The same resonator was loaded by another monopole antenna to cover the 5G mid-band cellular communications [7]. The design in [8] had two filters operating alternately to switch between the sensing mode and the communication mode of the CR system. The narrow band communication antenna of this design provides a continuous tuning over the WiMAX range. The same filters were attached to a circularly polarized wide slot antenna to provide continuous tuning for the communication antenna along the frequency range (2.44-3.19 GHz) [9]. A T-shaped resonator with a varactor diode was inserted within the feed line of a rectangular monopole antenna to provide continuous tuning over the range (1.68-1.73 GHz) [10].

The authors in [11] also proposed a combination of sensing and communication antennas but with step tuning communication mode switching between the WiMAX and the WLAN frequency bands. A quasi-Yagi filtering antenna was proposed in [12] to cover the 5G mid-band applications. Some non-planar structures were also used for the communication mode of the CR systems. A cavity backed filtering antenna was used to switch the communication mode from the narrow band to wideband [13]. A reconfigurable waveguide filtering antenna was proposed in [14] to provide step tuning along the X-band using a mechanical stepped metallic screws. A stacked filtering antenna was used with PIN diodes to generate a step tuning over the range (2.19-2.81 GHz) [15]. The reconfigurability of the communication filtering antenna was sometimes extended to switch the antenna polarization using a planar structure [16] or with the aid of a metasurface [17].

In this paper, a low cost reconfigurable filtering antenna is designed as a radiator for the communication mode of the CR system by combining a multi-mode resonator (MMR) with a wideband cup-shaped monopole antenna. The filtering antenna is tunable within the range (2.9-4 GHz) using step and continuous tuning modes. The step and continuous tuning serve the secondary user of the WiMAX CR system to communicate in the absence of the primary user at modifiable resonant frequencies and data rates. The step tuning is achieved by a pair of PIN diodes, while the continuous tuning is attained by a single varactor diode. When the PIN diodes are in their OFF state, the proposed filtering antenna operates with a tunable bandwidth along the frequency range (3.3-4 GHz), which is controlled by re-positioning the even mode resonant frequency depending on the value of the capacitance of the varactor diode. In adverse conditions, the ON state of the PIN diodes results in cancelling the even mode resonant frequency of the filtering antenna and shifting its odd mode resonance to the range (2.9-3.3 GHz). The out-of-band radiation has been significantly reduced by inserting two C-shaped parasitic elements. The resulted filtering antenna has a stable omnidirectional radiation pattern with reasonable gain values for all states of the PIN diodes and varactor diodes.

II. FILTERING ANTENNA STRUCTURE

The geometry of the proposed filtering antenna is illustrated in Figure 1. The structure consists of a cup-shaped planar monopole antenna attached to an E-shaped MMR with a pair of C-shaped parasitic elements and a pair of matching stubs. The antenna part is an ultra-wide band (UWB) with semi-circular patch terminated by a rectangular patch and partial ground plane. The E-shaped MMR is electromagnetically coupled with the feed line and the antenna. The length of the central arm of the E-shaped MMR is tuned by a varactor diode, while the presence and absence of the matching stubs are determined by a pair of PIN diodes. The dielectric substrate of the proposed antenna is an FR4 with dielectric constant of $\varepsilon_r = 4.3$, loss tangent of 0.025, and \\\height of $h = 1.6mm$. The overall dimension of the designed filtering antenna is $(40 \times 50 \times 1.6)\ mm^3$. The PIN diode used in this design is SMP1320-079L manufactured by SKYWORKS, while the varactor diode is BB857-02V manufactured by Infineon (BB85702VH7902XTSA1).

III. DESIGN STEPS

It is clear that the antenna used in the proposed design is an ultra-wideband monopole antenna, so it is important to determine its bandwidth within the intended band (the WiMAX band in this work) using a filter. The attached filter has been gradually designed to generate a controllable filtering antenna that is suitable for the communication part of the CR system. Figure 2 shows the steps that were followed to reach the final design of the filtering antenna, while Figure 3 exhibits the reflection coefficient corresponding to

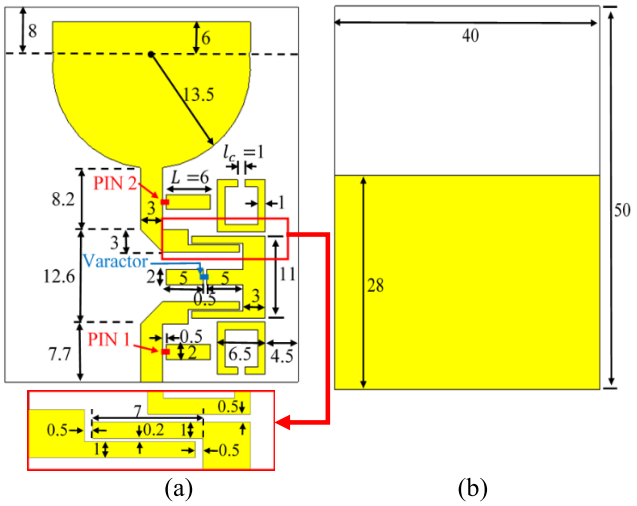

FIGURE 1. The geometry of the proposed filtering antenna (all dimensions are in mm).

each step. It is worth mentioning that the cup-shaped patch of the monopole antenna is selected to provide a quarter wavelength resonator with miniaturized dimensions because the area of its radiating patch is approximately half that of the conventional elliptical monopole antenna with the same first resonant frequency.

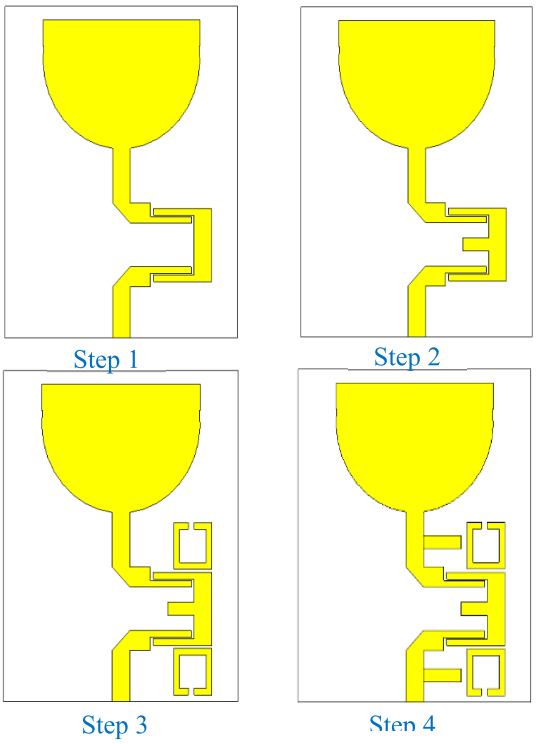

FIGURE 2. The design steps of the proposed filtering antenna.

Step 1: The design starts by attaching a conventional MMR resonator to the antenna, which results in multiple resonant frequencies covering a wide range of frequencies. The first and second resonant frequencies are the odd mode and even mode of the filtering antenna, respectively [18]. The rest resonant frequencies are the higher order odd and even mode frequencies arranged alternately along the operational band of the antenna.

Step 2: According to the even and odd mode analysis that will be explained in the next section, the presence of the central arm shifts down the even mode resonant frequency (second resonant frequency) with a subtle effect on the odd mode frequency (first resonant frequency). The resulted reflection coefficient has overlapped the even and odd resonant frequencies with undesired out-of- band matching.

Step 3: A pair of C-shaped parasitic elements is positioned close to the resonator to generate a transmission zero that eliminates the undesired matching of the higher order resonant frequencies. As shown in Figure 3, the resulted reflection coefficient in this step has no undesired matching at frequencies larger than 4.2 GHz.

Step 4: Adding a pair of matching stubs to the filtering antenna switches its operation to a completely different status. The antenna in this step is a single band antenna covering the lower range of the WiMAX frequency band because the matching stub is designed to enhance the matching of the odd mode resonant frequency and cancel the even mode frequency, as will be discussed in the next section.

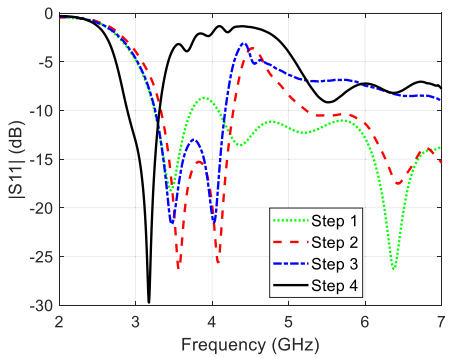

FIGURE 3. Simulated reflection coefficient corresponding to each design step.

As a result, the filtering antenna can operate as a wideband filtering antenna with controllable bandwidth in the absence of the matching stubs. On the other hand, its operation is switched to a single-band filtering antenna in the presence of the matching stubs. Therefore, the proposed filtering antenna can be modified to be a reconfigurable filtering antenna with continuous and step tuning to cover the WiMAX band, as will be revealed in Section IV.

IV. E-SHAPED MMR FILTER ANALYSIS

In order to understand the criterion of the proposed filtering antenna, it is important to analyze the E-shaped MMR because of its modifiable resonant frequencies. It is known that the analysis of the MMR is based on transmission line modeling, which is highly dependent on the microstrip line characteristic impedance and the effective dielectric constant of the dielectric substrate. Meanwhile, the values of the

characteristic impedance (Z_o) and the effective dielectric constant (ε_{re}) can be calculated from the well-known empirical equations given in [19], [20]. Furthermore, the input impedance (Z_{in}) of a lossless microstrip line terminated with a load (Z_L) is presented in [21]. The relationship between the phase constant (β) and the resonant frequency (f_r) can be found with the aid of the quasi-TEM behavior of the microstrip line as follows [21]:

$$\beta = 2\pi f_r \frac{\sqrt{\varepsilon}_{re}}{c} \tag{1}$$

where c is the speed of light in free space. The even and odd mode analysis [20], [21] is applied to the proposed E-shaped MMR to give a criterion about the locations of the resonant frequencies of the resonator. Figure 4 reveals the E-shaped resonator with its odd mode and even mode equivalent structures.

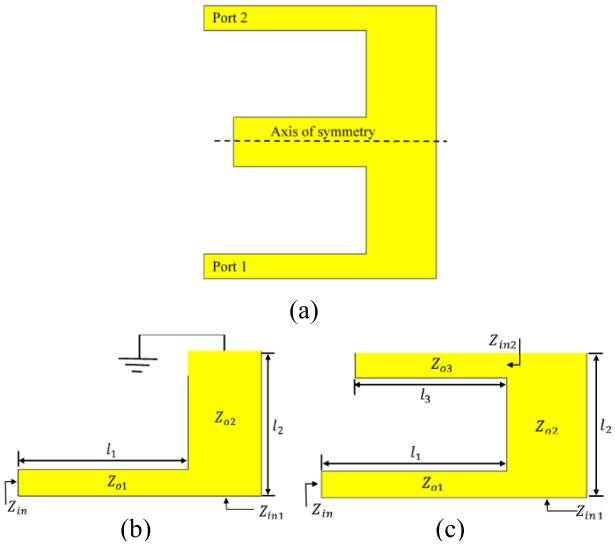

FIGURE 4. Even and odd modes analyses (a) E-shaped MMR, (b) odd mode, and (c) even mode.

A. ODD-MODE RESONANT FREQUENCY

By feeding the resonator ports from two sources with equal amplitudes and 180° phase difference, the odd mode of the MMR is obtained. At the resonant frequency, the voltage signals of the two sources meet each other at the axis of symmetry [see Figure 4(a)] with equal amplitudes and 180° phase difference, whereas the current signals at the axis of symmetry have equal amplitudes and 0° phase difference. Consequently, the current is maximum and the voltage is zero at the axis of symmetry, which is exactly equivalent to a short circuit. Therefore, the center arm is negligible and has no effect on the odd resonant frequency in this case, and the odd mode equivalent structure is as shown in Figure 4(b). The characteristic impedances of the first and second pieces of the odd mode E-shaped MMR are Z_{o1} and Z_{o2}. In addition, their lengths are equal to l_1 and l_2, respectively. The input impedance (Z_{in1}) of the short circuit line is given by:

$$Z_{in1} = jZ_{o2}\ tan\ (\beta l_2) \tag{2}$$

Using Z_{in1} as a load for the feeding transmission line, the input impedance (Z_{in}) of the odd mode circuit is given by:

$$Z_{in} = Z_{o1}\frac{Z_{in1} + jZ_{o1}tan\ (\beta l_1)}{Z_{o1} + jZ_{in1}tan\ (\beta l_1)} \tag{3}$$

At the resonant frequency, the value of the input impedance approaches to infinity ($Z_{in} = \infty$) [22]. Therefore, by equating the denominator of (3) to zero and substituting the value of Z_{in1} from (2), the resonance condition will be as follows:

$$Z_{o1} - Z_{o2}tan\ (\beta l_2)\ tan\ (\beta l_1) = 0 \tag{4}$$

Using a simple computer code, the value of (β) can be found in terms of Z_{o1}, Z_{o2}, l_1, and l_2. Then, the odd resonant frequency (f_{ro}) can be calculated using (1).

B. EVEN-MODE RESONANT FREQUENCY

This mode is attained by feeding the two ports of the E-shaped MMR with two sources with equal amplitudes and a zero phase difference. As a result, the voltages at the plane of symmetry have equal amplitudes and equal phase angles, while the currents are with equal amplitudes and 180° phase difference. In this case, the axis of symmetry is equivalent to an open circuit, so the effect of the central arm of the E-shaped MMR on the even resonant frequency can clearly be sensed under this condition, as shown in Figure 4(c).

The input impedance of the open circuit line (Z_{in3}) is given by the following equation:

$$Z_{in2} = -jZ_{o3}\ cot\ (\beta l_3) \tag{5}$$

where Z_{o3} and l_3 represent the characteristic impedance and the length of the open circuit line, respectively. Thus,

$$Z_{in1} = Z_{o2}\frac{Z_{in2} + jZ_{o2}tan\ (\beta l_2)}{Z_{o2} + jZ_{in2}tan\ (\beta l_2)} \tag{6}$$

The input impedance equation of the even mode is given above in (3). The same as in the odd mode case, the even mode resonant frequency results in input resistance equal to infinity, so the resonance condition can be rewritten as follows:

$$Z_{o1} + jZ_{o2}\frac{-jZ_{o3}\ cot\ (\beta l_3) + jZ_{o2}tan\ (\beta l_2)}{Z_{o2} + Z_{o3}\ cot\ (\beta l_3)\ tan\ (\beta l_2)}tan\ (\beta l_1) = 0 \tag{7}$$

Similarly, by finding the value of (β) in term of (Z_{o1}, Z_{o2}, Z_{o3}, l_1, l_2, and l_3), the value of the even mode resonant frequency (f_{re}) can be deduced from (1).

In conclusion, the length of the central arm of the E-shaped MMR determines the value of the even resonant frequency, but it has a very negligible effect on the odd resonant frequency. Therefore, the electrical length of the central arm can be tuned by a varactor diode to obtain variable even mode resonant frequency that can be utilized for a filtering antenna with tunable bandwidth.

To verify the aforementioned claims, the current distribution of the proposed E-shaped MMR at the odd-mode resonant frequency (3.54 GHz) and the even-mode resonant frequency (3.9 GHz) is illustrated in Figure 5. It clear that Figure 5(a) shows a negligible amount of current at the central arm of the MMR. On the other hand, the current is heavily concentrated at the central arm of the MMR at the even-mode resonant frequency as shown in Figure 5(b).

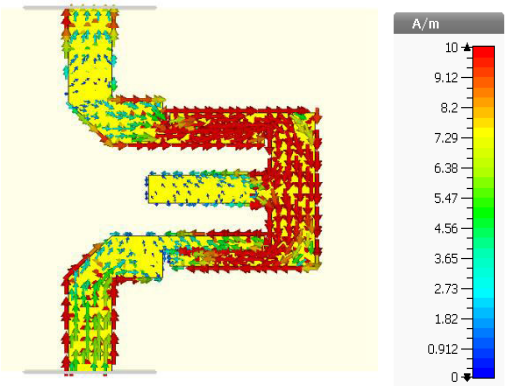

(a)

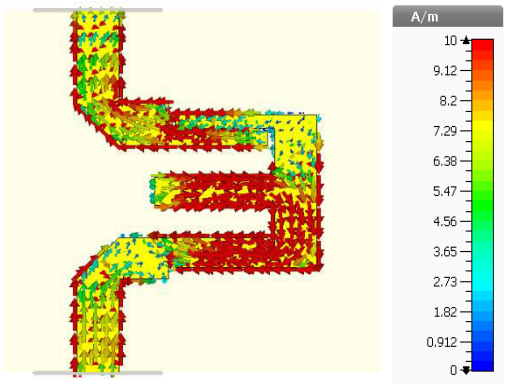

(b)

FIGURE 5. Surface current distribution of the proposed E-shaped MMR at (a) the odd-mode resonant frequency 3.54 GHz and (b) even-mode resonant frequency 3.9 GHz.

The equivalent circuit of the proposed E-shaped MMR band-pass filter is illustrated in Figure 6. The lower LC circuits is responsible for the odd-mode resonation of the filter, while the upper LC circuit generates the even-mode of the filter. L_{odd} and L_{even} represents the inductance of the odd and even mode resonant circuits, respectively. On the other hand, C_{odd} and C_{even} are the capacitance of the odd and even mode resonant circuits, respectively. For the odd-mode analysis, the resonant frequency (f_{ro}) and quality factor (Q_{odd}) are given below in (8) and (9), respectively.

$$f_{ro} = \frac{1}{2\pi\sqrt{L_{odd}C_{odd}}} \tag{8}$$

$$Q_{odd} = \frac{2\pi f_{ro}L_{odd}}{R_o} \tag{9}$$

Similarly, the even-mode resonant frequency (f_{re}) and quality factor (Q_{even}) are given below in (10) and (11), respectively.

$$f_{re} = \frac{1}{2\pi\sqrt{L_{even}C_{even}}} \tag{10}$$

$$Q_{odd} = \frac{2\pi f_{re}L_{even}}{R_o} \tag{11}$$

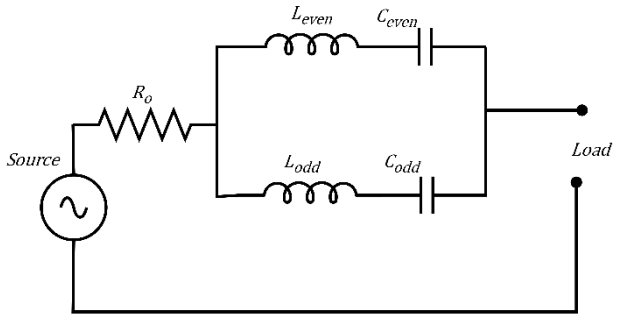

FIGURE 6. Equivalent circuit diagram of the proposed E-shaped MMR filter.

V. SIMULATION RESULTS

The simulation results of the proposed design were acquired using the CST microwave studio simulation suite [23]. The PIN diodes that were used in this work are both SMP1320-079L (manufactured by Skyworks), whose forward biasing parameters are 0.9Ω resistor and 0.7 nH inductor, while their reverse biasing capacitance value is 0.23 pF capacitor. The varactor diode used in this work is BB857-02V, manufactured by Infineon (BB85702VH7902XTSA1). The series resistance of this varactor diode is equal to 1.5Ω, whereas its reverse biasing capacitance range extends from 0.52 pF (at 28 V) up to 7.2 pF (at 1 V).

As shown earlier in Figure 1, the PIN diodes are mounted on both matching stubs of the filter part to switch their presence and absence. On the other hand, the varactor diode is placed on the central arm of the E-shaped MMR. Both PIN diodes are switched ON and OFF simultaneously to provide step switching, while the continuous tuning is provided by the varactor diode.

A. REVERSE BIASING OF THE PIN DIODES

When the two PIN diodes are at their OFF state, the two matching stubs are detached from the structure of the filtering antenna. In this case, both the even and odd mode resonant frequencies are matched properly. As mentioned in the previous Section III, the location of the even resonant frequency can be tuned by changing the capacitance value of the varactor diode because this variation results in controlling the electrical length of the central arm of the E-shaped MMR. In adverse conditions, the odd resonant frequency is unaffected by this variation. Figure 7 illustrates the reflection coefficient of the designed filtering antenna for different varactor capacitance values when the PIN diodes are in their OFF state. It is clear that the antenna covers the upper range

of the WiMAX frequency band with a tunable bandwidth. It can clearly be seen that the odd resonant frequency is fixed at about 3.54 GHz. The widest bandwidth is when the capacitance value is equal to 1 pF, which is equal to 750 MHz ($3.3 - 4.05$ GHz), and the narrowest bandwidth is 300 MHz ($3.3 - 3.65$ GHz) when the capacitance is equal to 7 pF.

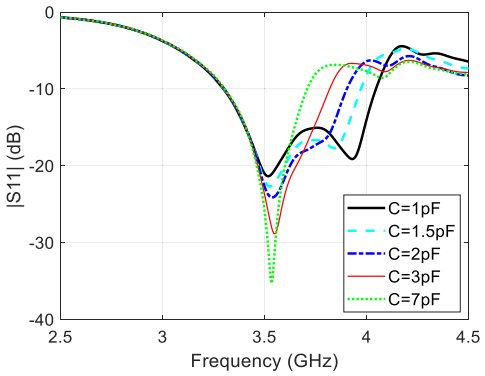

FIGURE 7. Simulated reflection coefficient of the proposed filtering antenna when the PIN diodes are at OFF states with $L = 6mm$, $l_c = 1mm$, and different values of varactor capacitance (C).

The presence of the C-shaped parasitic elements in the vicinity of the MMR is responsible for eliminating the undesired out-of-band matching as explained previously in Section III. The band notch generation parasitic elements are categorized into half wavelength parasitic elements and quarter wavelength parasitic elements [24]. The C-shaped parasitic element in this work is a half wavelength band notch generator. Therefore, controlling the length of this element results in controlling the location of the notched band along the frequency axis. In this work, the distance between the terminals of the C-shaped parasitic element (l_c) is changed to identify the suitable location of the band notch that results in the cancellation of the undesired matching at frequencies larger than the upper edge of the filtering antenna bandwidth. The length of the parasitic element decreases as l_c increases, so the location of the notched band is shifted to higher frequencies as exhibited in Figure 8. For $l_c = 0.5mm$, the notched frequency is located within the antenna bandwidth at $4GHz$. Although $l_c = 1.5mm$ gives good cancelation for the unwanted out-of-band matching, $l_c = 1mm$ is considered the most suitable value because it gives a higher reflection coefficient value (better out-of-band cancelation).

B. FORWARD BIASING OF THE PIN DIODES

The ON state of the PIN diodes results in the insertion of the matching stubs to the E-shaped MMR. The matching stubs are designed to match the odd resonant frequency while mismatching the even resonant frequency. In addition, they shift the odd resonant frequency down to about 3.2 GHz because the matching stubs modify the input impedance of the filter, which results in modifying the resonation condition given in equation (4). Figure 9 illustrates the reflection coefficient of

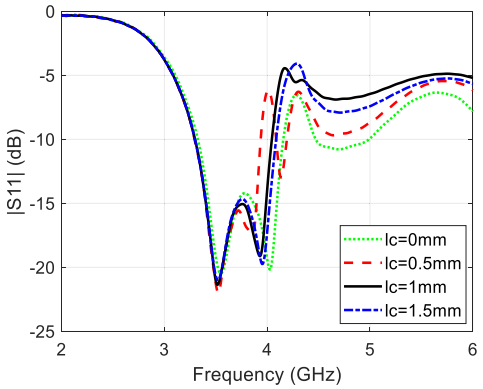

FIGURE 8. Simulated reflection coefficient of the proposed filtering antenna when the PIN diodes are at OFF states with $L = 6mm$, $C = 1pF$, and different values of l_c.

the proposed filtering antenna for different capacitance values with ON state of PIN diodes.

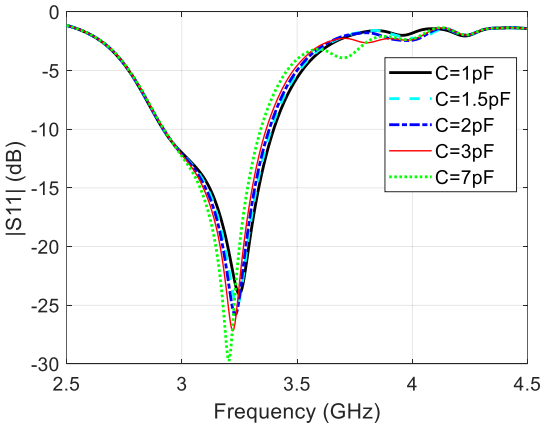

FIGURE 9. Simulated reflection coefficient of the proposed filtering antenna when the PIN diodes are at ON states with $L = 6mm$, $l_c = 1mm$, and different values of varactor capacitance (C).

Figure 10 verifies the presence of the odd mode resonant frequency because the variation of the capacitance has a trivial effect on the location of the resonant frequency, and this is what has also been proved in the previous Subsection A. The resulted antenna bandwidth is 400 MHz along the range ($2.9 - 3.3$ GHz) at $C = 7pF$, which represents the lower range of the WiMAX frequency band. The effect of the length of the matching stub (L) is also tested to find the suitable value that leads to perfect cancellation for the even resonant frequency of the filtering antenna. It can be seen in Figure 10 that the cancellation of the even mode resonant frequency is improved as L increases. Besides, the position of the odd mode frequency is modified during the variation of the stub length, and this verifies the deduction of the effect of the presence of the stub on the resonation condition. $L = 6mm$ is the most suitable value because it results in a strong mismatch in the out-of- band range of frequencies, and the separation between the C-shaped element and the matching stub is still reasonable at this value of L.

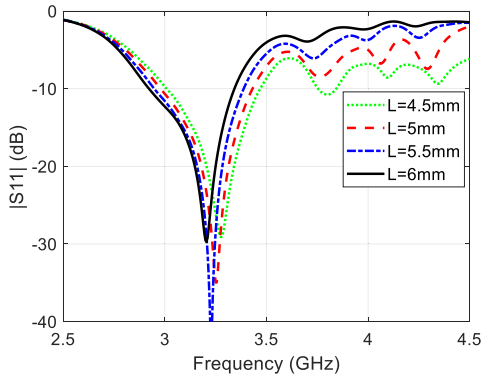

FIGURE 10. Simulated reflection coefficient of the proposed filtering antenna when the PIN diodes are at ON states with $C = 7pF$, $l_c = 1mm$, and different values stub length (L).

Finally, to verify the isolation of the filter, it is important to demonstrate the simulated realized gain of the resulted filtering antenna. Figure 11 demonstrates the simulated realized gain of the antenna without filter, the filtering antenna with PIN diodes OFF, and the filtering antenna with PIN diodes ON

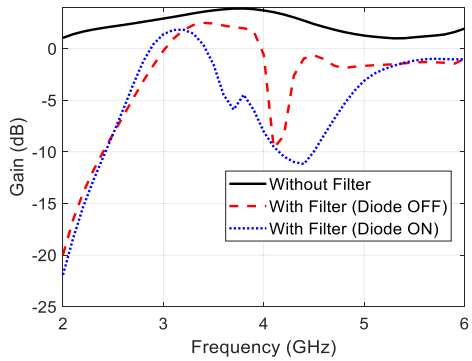

FIGURE 11. Comparison of the simulated realized gain of the antenna without filter with that of the filtering antenna with PIN diodes (ON and OFF states) with varactor diode capacitance $C = 1pF$.

It can be seen that the presence of the filter significantly reduces the antenna gain at frequency ranges outside the pass band of the filter to values less than 0 dB. It is worth mentioning that the internal resistances of the PIN diodes and the varactor accumulate additional losses that results in increasing the insertion loss of the E-shaped MMR. As a result, the antenna realized gain is reduced after inserting these switching elements.

VI. MEASUREMENT RESULTS

Figure 12 shows the prototype of the proposed reconfigurable filtering antenna, whereas Figure 13 shows a photograph of the reflection coefficient measurement equipment setup. The filtering antenna is fabricated on an FR4 substrate with a dielectric constant of $\varepsilon_r = 4.3$, a loss tangent of 0.025, and a height of $h = 1.6mm$. The PIN diodes used in this design are SMP1320-079L (manufactured by Skyworks), and the varactor diode is BB857-02V manufactured by Infineon (BB85702VH7902XTSA1). The diodes internal elements values are previously mentioned in details in Section V. Three external 10 nH chocking inductors are inserted at the biasing lines to protect the DC source from the high frequency signal of the network analyzer. Furthermore, additional protection for the diode is provided by connecting the biasing lines of the antenna to external 1 kΩ resistors to restrict the current passing through them.

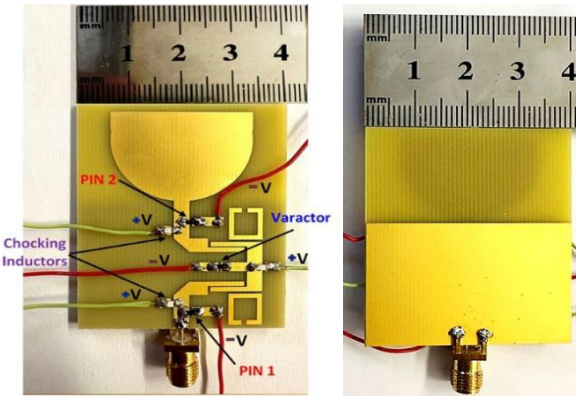

FIGURE 12. Prototype of the proposed filtering antenna (a) front view and (b) back view.

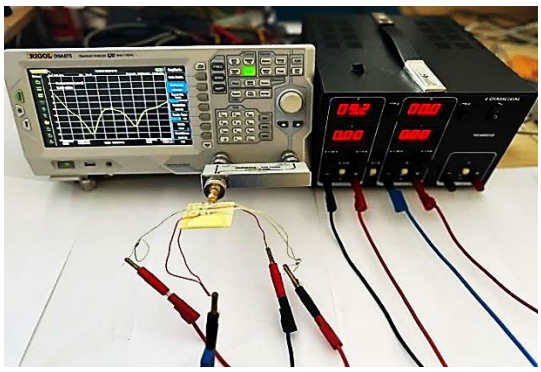

FIGURE 13. Reflection coefficient measurement equipment setup.

A. MEASUREMENTS AT THE PIN DIODE OFF STATE

Figure 14(a) illustrates the simulation reflection coefficients of the designed reconfigurable filtering antenna at the OFF state of the PIN diodes and the variable capacitance values of the varactor diode. Figure 14(b) reveals the measured reflection coefficient when the PIN diodes are at their OFF state and at different reverse biasing voltages of the varactor diode. The reverse biasing voltages were selected to give approximately the same capacitance values as presented in the simulation results. The measurements clearly verify the variable bandwidth of the proposed filtering antenna within the upper range of the WiMAX frequency range. The simulated (measured) tunable bandwidth of the filtering antenna in this case extends

along the range $3.3-4.05\ GHz$ ($3.25-4.02\ GHz$) down to the range $3.3-3.65\ GHz$ ($3.25-3.58\ GHz$). The deviation between the measured and simulated results comes from many factors, such as the imperfect soldering of the SMA connector and the diodes, the fabrication imperfection, and the effect of the presence of the biasing lines.

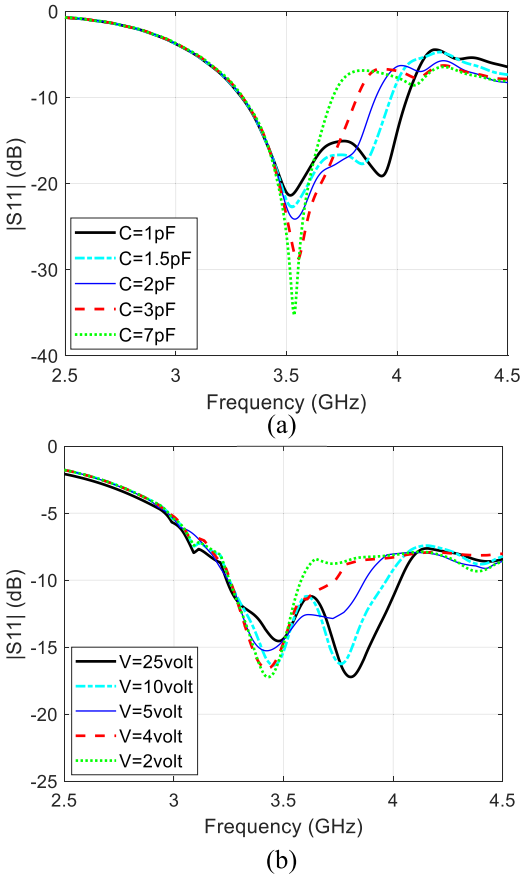

FIGURE 14. Reflection coefficient of the proposed filtering antenna when PIN diode at OFF state and variable capacitance (reverse biasing voltage) values of the varactor diodes (a) simulated and (b) measured.

It is worth mentioning that the radiation characteristics of the filtering antenna at the OFF state of the PIN diodes were studied at a capacitance value equal to 1 *pF* (25 *V* reverse biasing voltage) because it gave the widest bandwidth compared to the other values. Therefore, the variation of the antenna radiation characteristics is expected to be the largest compared to that of the other capacitance values. Figure 15 shows the power pattern of the proposed filtering antenna at the resonant frequencies when the PIN diodes are at the OFF state and capacitance value of the varactor diode equal to 1 *pF* (25 *V* reverse biasing voltage). For both resonant frequencies, the power pattern of the antenna is omnidirectional, which is suitable for portable CR devices.

The simulated and measured gains of the reconfigurable filtering antenna at PIN diodes OFF state and capacitance values equal to 1 *pF* (25 *V* reverse biasing voltage) are illustrated in Figure 16. It is clear that the E-shaped MMR

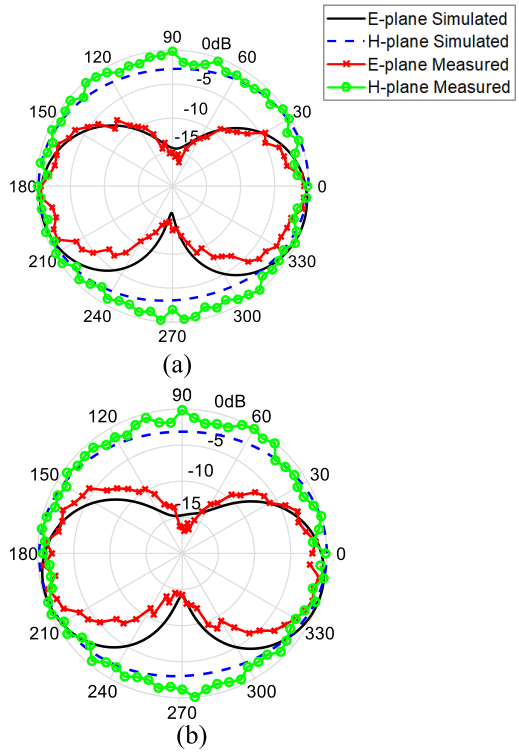

FIGURE 15. Simulated and measured power patterns of the proposed filtering antenna when PIN diode at OFF state and varactor diode capacitance value equal to 1 pF at frequency equal to (a) f=3.54 GHz and (b) f=3.9 GHz.

determines the gain value to be larger than 0 *dB* within its pass band and suppresses the gain to values less than 0 *dB* at its stop bands. The maximum simulated (measured) gain value is 2.5 *dBi* (2.48 *dBi*).

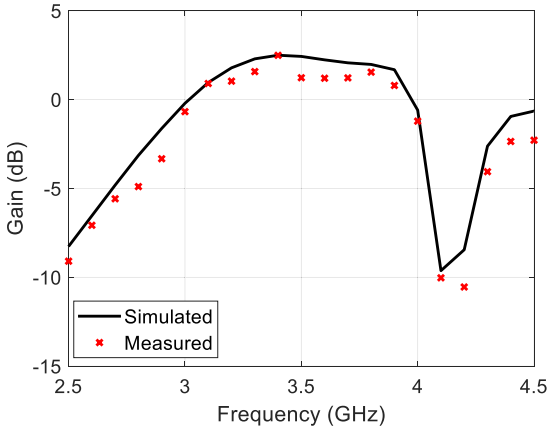

FIGURE 16. Simulated and measured gain of the proposed filtering antenna when PIN diode at OFF state and varactor diode capacitance value equal to 1 pF.

The fluctuations of the measured power pattern and gain are attributed to the reflections coming back from the surrounding objects inside the anechoic chamber. However, the general forms of the measured power pattern and the realized

TABLE 1. Comparison between the proposed filtering antenna with other important filtering antennas, where λ_o is the wavelength corresponding to the lowest resonant frequency of the antenna.

Ref.	Ant. Dimensions	Step tuning / freq.s (GHz)	Continuous tuning / freq. Range (GHz)	Max. Gain (dB)	Rad. Pattern
[4]	$0.61\lambda_o \times 1.215\lambda_o \times 0.0325\lambda_o$	-	6.16-6.47	6.77	Directional
[5]	$0.62\lambda_o \times 1.23\lambda_o \times 0.033\lambda_o$	-	6.2-6.5	5.62	Directional
[7]	$0.32\lambda_o \times 0.3\lambda_o \times 0.0165\lambda_o$	-	3.6-3.8	1.9	Omni-directional
[10]	$0.568\lambda_o \times 0.568\lambda_o \times 0.009\lambda_o$	-	4.26-5.94	2.3	Omni-directional
[11]	$0.364\lambda_o \times 0.5408\,\lambda_o \times 0.016\lambda_o$	3.6, 5.2	-	2.48	Omni-directional
[12]	$0.935\lambda_o \times 0.385\lambda_o \times 0.0176\lambda_o$	-	3.3-3.8	4.73	Directional
[14]	$0.43\lambda_o \times 0.27\lambda_o \times 0.2\lambda_o$	-	8.1-9.2	5.8	Directional
[15]	$1\lambda_o \times 0.66\lambda_o \times 0.036\lambda_o$	-	2.19-2.81	4.9	Directional
This work	$\mathbf{0.413\lambda_o \times 0.516\lambda_o \times 0.0165\lambda_o}$	**3.1, 3.54**	**3.26-4.02**	**2.5**	**Omni-directional**

gain are close to the simulated ones because the switching elements and their biasing lines are positioned on the filter part of the antenna. This is one of the main advantages of the reconfigurable filtering antennas over the conventional reconfigurable antennas, whose reconfigureble elements and biasing lines heavily distort the antenna radiation patterns.

B. MEASUREMENTS AT THE PIN DIODE ON STATE

As explained previously, the ON state of the PIN diodes results in a single band filtering antenna covering the lower range of the WiMAX band. Figure 17 shows the experimental verification of this claim where the simulated (measured) reflection coefficient shows filtering antenna bandwidth that covers the range $2.9 - 3.3\ GHz$ ($2.9 - 3.28\ GHz$). The measured reflection coefficient deviates from the simulated one due to the imperfect soldering of the SMA connector and diodes as well as the inaccuracy of the fabrication

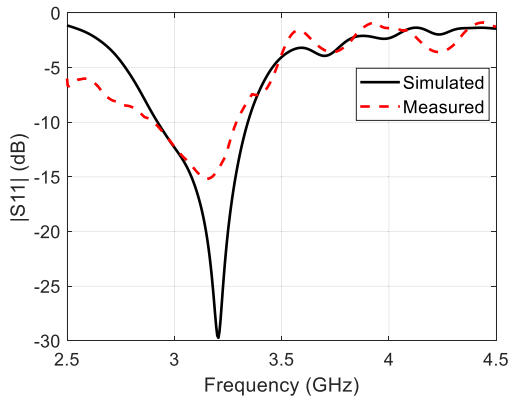

FIGURE 17. Reflection coefficient of the proposed filtering antenna when PIN diode at ON state and varactor diode capacitance value equal to 7pF (reverse biasing voltage 2V).

The simulated and measured power patterns of the proposed filtering antenna when the PIN diodes are at their ON state and the varactor diode capacitance value equal to $7\ pF$ ($2\ V$ reverse biasing voltage) are shown in Figure 18. The antenna also shows an omnidirectional pattern suitable for portable CR gadgets. Under the same conditions, the simulated and measured gains are evaluated and shown in Figure 19. The filtering antenna has gain values larger than $0\ dB$ within the pass band of the E-shaped MMR. The radiation characteristics have small fluctuations due to the waves reflecting back from the surrounding objects, but the overall shapes of the power patterns and gain are almost similar to their simulated counterparts because the switching elements are mounted on the filter away from the antenna radiating patch.

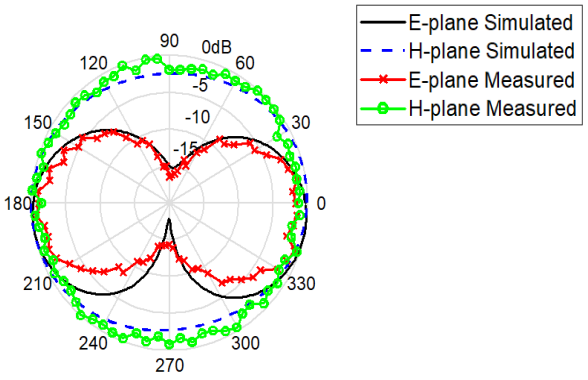

FIGURE 18. Simulated and measured power patterns of the proposed filtering antenna when PIN diode at ON state and varactor diode capacitance value equal to 7pF (reverse biasing voltage 2V).

The results show the importance of the proposed filtering antenna in the WiMAX CR systems. The design serves the secondary user of the CR system to communicate in the absence of the primary users at different data rates and different resonant frequencies. Once the primary user appears, the secondary user is switched to another frequency band or operate with reduced bandwidth to avoid interfering with the primary user.

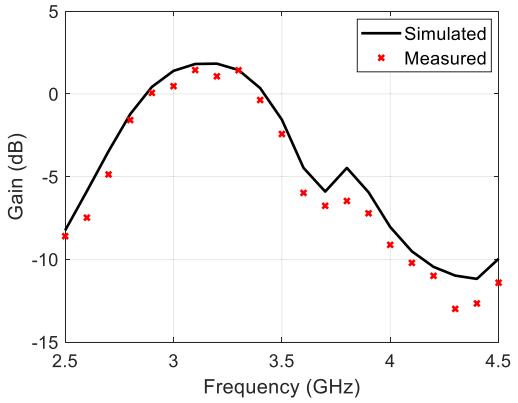

FIGURE 19. Simulated and measured gain of the proposed filtering antenna when PIN diode at ON state and varactor diode capacitance value equal to 7pF (reverse biasing voltage 2V).

Table 1 compares the proposed filtering antenna with some other important filtering antennas that are used as communication antennas for CR systems. To give a fair comparison, the antenna dimensions are normalized to the wavelength (λ_o) corresponding to the lowest resonant frequency of the antenna. Compared to the other designs, this table reveals that the proposed filtering antenna has the smallest dimensions, with a very acceptable maximum gain value, and an omnidirectional radiation pattern suitable for portable devices. In addition, the table also shows the superiority of the proposed filtering antenna in providing both step and continuous tuning mechanisms unlike the other designs which have either step or continuous tuning.

VII. CONCLUSION

In this work, a compact reconfigurable filtering antenna with step and continuous tuning capabilities that can be utilized for the communication part of the CR systems has successfully been designed. The structure of the proposed design consists of a cup-shaped monopole antenna and an E-shaped MMR. The step tuning is achieved with the aid of a pair of PIN diodes that can switch the operation of the antenna from a lower frequency range of WiMAX to its upper range and vice versa. The off state of the PIN diodes results in the presence of a fixed odd mode frequency and an even mode resonant frequency whose value can continuously be tuned by a varacter diode. This state of PIN diodes presents a variable simulated (measured) bandwidth with an upper range of 3.3-4.05 GHz (3.25-4.02 GHz) and a lower range of 3.3-3.65 GHz (3.25-3.58 GHz). During the ON state of the PIN diodes, the filtering antenna operates as a single band antenna along the simulated (measured) range 2.9-3.3 GHz (2.9-3.28 GHz) due to the cancellation of the even mode resonation while keeping the fixed odd mode resonation. In both modes, the power pattern of the antenna is omnidirectional with simulated (measured) maximum gain value equal to 2.5 dB (2.48 dB). The results also show gain values larger than 0 dB within the pass band of the MMR, while the gain values are weak along the stop band of the resonator.

REFERENCES

[1] Y. Tawk, J. Costantine, and C. Christodoulou, *Antenna Design for Cognitive Radio*. Norwood, MA, USA: Artech House, 2016.
[2] F. M. Alnahwi, A. Abdulhameed, and A. S. Abdullah, "A compact integrated UWB/reconfigurable microstrip antenna for interweave cognitive radio applications," *Int. J. Commun. Antenna Propag. (IRECAP)*, vol. 8, no. 1, p. 81, Feb. 2018.
[3] F. M. Alnahwi, A. A. Abdulhameed, H. L. Swadi, and A. S. Abdullah, "A planar integrated UWB/reconfigurable antenna with continuous and wide frequency tuning range for interweave cognitive radio applications," *Iranian J. Sci. Technol., Trans. Electr. Eng.*, vol. 44, no. 2, pp. 729–739, Jun. 2020.
[4] Y. Tawk, J. Costantine, and C. G. Christodoulou, "A varactor-based reconfigurable filtenna," *IEEE Antennas Wireless Propag. Lett.*, vol. 11, pp. 716–719, 2012.
[5] Y. Tawk, M. E. Zamudio, J. Costantine, and C. G. Christodoulou, "A cognitive radio reconfigurable 'filtenna,'" in *Proc. 6th Eur. Conf. Antennas Propag. (EUCAP)*, Mar. 2012, pp. 3565–3568.
[6] M.-C. Tang, Y. Chen, and R. W. Ziolkowski, "Experimentally validated, planar, wideband, electrically small, monopole filtennas based on capacitively loaded loop resonators," *IEEE Trans. Antennas Propag.*, vol. 64, no. 8, pp. 3353–3360, Aug. 2016.
[7] F. K. Juma'a, A. I. Al-Mayoof, A. A. Abdulhameed, F. M. Alnahwi, Y. I. A. Al-Yasir, and R. A. Abd-Alhameed, "Design and implementation of a miniaturized filtering antenna for 5G mid-band applications," *Electronics*, vol. 11, no. 19, p. 2979, Sep. 2022.
[8] M.-C. Tang, Z. Wen, H. Wang, M. Li, and R. W. Ziolkowski, "Compact, frequency-reconfigurable filtenna with sharply defined wideband and continuously tunable narrowband states," *IEEE Trans. Antennas Propag.*, vol. 65, no. 10, pp. 5026–5034, Oct. 2017.
[9] Z. Wen, M. Tang, and R. W. Ziolkowski, "Band- and frequency-reconfigurable circularly polarised filtenna for cognitive radio applications," *IET Microw., Antennas Propag.*, vol. 13, no. 7, pp. 1003–1008, Jun. 2019.
[10] H. A. Atallah, A. B. Abdel-Rahman, K. Yoshitomi, and R. K. Pokharel, "Compact frequency reconfigurable filtennas using varactor loaded T-shaped and H-shaped resonators for cognitive radio applications," *IET Microw., Antennas Propag.*, vol. 10, no. 9, pp. 991–1001, Jun. 2016.
[11] Y. M. Hasan, A. S. Abdullah, and F. M. Alnahwi, "Dual-port filtenna system for interweave cognitive radio applications," *Iranian J. Sci. Technol., Trans. Electr. Eng.*, vol. 46, no. 4, pp. 943–958, Dec. 2022.
[12] L. Zhai, Y. Guo, Z. Xu, X. Zhang, Y. Chen, and J. Shi, "Designing a compact filtering quasi-Yagi antenna with multiple radiation nulls using embedded resistor-loaded arms," *Micromachines*, vol. 14, no. 7, p. 1445, Jul. 2023.
[13] Y.-M. Wu, S.-W. Wong, H. Wong, and F.-C. Chen, "A design of bandwidth-enhanced cavity-backed slot filtenna using resonance windows," *IEEE Trans. Antennas Propag.*, vol. 67, no. 3, pp. 1926–1930, Mar. 2019.
[14] D. Singhal, S. S. Chauhan, and K. Dhwaj, "Compact reconfigurable waveguide filtering antenna," *IEEE Antennas Wireless Propag. Lett.*, vol. 22, no. 2, pp. 392–396, Feb. 2023.
[15] C. Guo, Z. Zhang, X. Fu, and J. Wang, "A frequency-reconfigurable antenna with filtering characteristics using characteristic mode analysis," *IEEE Antennas Wireless Propag. Lett.*, vol. 22, no. 8, pp. 1793–1797, Aug. 2023.
[16] M.-C. Tang, D. Li, X. Chen, Y. Wang, K. Hu, and R. W. Ziolkowski, "Compact, wideband, planar filtenna with reconfigurable tri-polarization diversity," *IEEE Trans. Antennas Propag.*, vol. 67, no. 8, pp. 5689–5694, Aug. 2019.
[17] L. Li, Z. Wu, Y. H. Huang, W. Wu, Q. X. Ma, J. J. Liang, and L. L. Huang, "Wideband and low-profile multi-polarization reconfigurable filtering antenna based on non-uniform Metasurface," *IEEE Trans. Compon., Packag., Manuf. Technol.*, vol. 13, no. 6, pp. 873–877, Jun. 2023.
[18] F. M. Alnahwi, Y. I. A. Al-Yasir, A. A. Abdulhameed, A. S. Abdullah, and R. A. Abd-Alhameed, "A low-cost microwave filter with improved passband and stopband characteristics using stub loaded multiple mode resonator for 5G mid-band applications," *Electronics*, vol. 10, no. 4, p. 450, Feb. 2021.
[19] C. A. Balanis, *Antenna Theory: Analysis and Design*. Hoboken, NJ, USA: Wiley, 2016.
[20] R. Garg, I. Bahl, and M. Bozzi, *Microstrip Lines and Slotlines*. Norwood, MA, USA: Artech House, 2013.
[21] D. M. Pozar, *Microwave Engineering*. Hoboken, NJ, USA: Wiley, 2011.

[22] S. Sun and L. Zhu, "Capacitive-ended interdigital coupled lines for UWB bandpass filters with improved out-of-band performances," *IEEE Microw. Wireless Compon. Lett.*, vol. 16, no. 8, pp. 440–442, Aug. 2006.
[23] *CST Microwave Studio*, MathWorks, Natick, MA, USA, 2014.
[24] F. M. Alnahwi and N. E. Islam, "A generalized concept for band notch generation in ultra-wide band antennas," *Prog. Electromagn. Res. C*, vol. 54, pp. 179–185, 2014.

FALIH M. ALNAHWI received the B.Sc. and M.Sc. degrees from the University of Basrah, Iraq in 2004 and 2007, respectively, and the Ph.D. degree in electrical and computer engineering from the University of Missouri, Columbia, MO, USA, in 2015. In 2015, he joined the Department of Electrical Engineering, University of Basrah, as a Lecturer, where he is currently an Associate Professor and the Director of Graduate Students. His research interests include antennas and wireless propagation especially multiband, broadband, ultra-wideband antennas, electromagnetic fields, MIMO systems, metamaterial, mutual coupling reduction techniques, reconfigurable antennas, microwave filter design, digital communications, optimization, and electromagnetic compatibility.

ABDULGHAFOR A. ABDULHAMEED received the B.Sc. degree in electrical engineering and the M.Sc. degree in electronics and communications engineering from the University of Basrah, in 2013 and 2016, respectively. He is currently pursuing the Ph.D. degree with the Department of Electronics and Information Technology, Faculty of Electrical Engineering, University of West Bohemia. In 2017, he joined the Department of Electrical Techniques, Qurna Technique Institute, Southern Technical University, as an Assistant Lecturer. His research interests include antenna design and analysis, microwave technology, electromagnetic fields, MIMO systems, metamaterials, mutual coupling reduction techniques, and electromagnetic compatibility.

NAZAR T. ALI (Senior Member, IEEE) received the Ph.D. degree in electrical and electronic engineering from the University of Bradford, U.K., in 1990. From 1990 to 2000, he was a Researcher and a Lecturer with the University of Bradford. He is currently an Associate Professor with Khalifa University, United Arab Emirates. He worked in many collaborative research projects in the U.K. under the umbrella of the Centre of Research Excellence, Department of Trade and Industry (DTI) and EPSERC. This involved a consortium of a number of universities and industrial companies. He has more than 100 papers published in peer-reviewed high-quality journals and conferences. His current research interests include antennas and RF circuits and systems, indoor and outdoor localization techniques, and RF measurements.

YASIR I. A. AL-YASIR (Member, IEEE) received the B.Sc. and M.Sc. degrees from the University of Basrah, in 2012 and 2015, respectively, and the Ph.D. degree from the University of Bradford, in 2021. In 2014, he joined the Antennas and RF Engineering Research Group, University of Bradford, as a Research Visitor. From 2018 to 2020, he was a Marie Curie Research Fellow with the University of Bradford, involved in the H2020-ITN-SECRET Project targeting 5G mobile small cells and funded by the EU Commission. He was a Research Fellow with the Faculty of Engineering and Informatics, University of Bradford, involved in the SATNEX-V Project, funded by the European Space Agency. He is currently a Research and Development Engineer working in the RF, Telecommunication and Space Industry, U.K. He has authored two books and ten book chapters and published more than 140 journal and conference papers on aspects of RF and microwave engineering. His articles have more than 2900 citations with an H-index of 28 and an i10-index of 61, as reported by Google Scholar. He was a recipient and co-recipient of various awards and prizes, such as the Best Paper Award from the IEEE 2nd 5G World Forum and IEEE 4th 5G Summit Dresden, Germany. He is a reviewer of various high-ranking journals and publishers, such as IEEE, IET, Wiley, Springer, Elsevier, and MDPI.

ZDENĚK KUBÍK was born in Planá, Czech Republic, in 1982. He received the Ph.D. degree in electrical engineering from the University of West Bohemia (UWB), Pilsen, Czech Republic, in 2012. He is currently a Lecturer with the Department of Applied Electronics and Telecommunications, UWB. His research interests include EMC measurement, developing new measurement techniques and electromagnetic, computational electromagnetics, electromagnetic fields wave propagation, finite element method, and antenna.

ABDULKAREEM S. ABDULLAH (Senior Member, IEEE) received the B.Sc. and M.Sc. degrees in communication engineering from the College of Engineering, University of Basrah, in 1980 and 1985, respectively, the Ph.D. degree in electromagnetic fields and microwaves technology from the Beijing University of Posts and Telecommunications (BUPT), Beijing, China, in 2004, and the Postdoctoral degree in telecommunications engineering from the Beijing Institute of Technology, China, in 2008. He is currently a Professor with the Department of Electrical Engineering, College of Engineering, University of Basrah. He has published more than 100 journal and conference papers. His research interests include antenna design and analysis, smart antennas, microwave technology, and indoor and outdoor radio wave propagation.

RAED A. ABD-ALHAMEED (Senior Member, IEEE) has been a Research Visitor with Wrexham University, Wales, since 2009, covering the wireless and communications research areas, and an Adjunct Professor with the College of Electronics Engineering, Ninevah University, since 2019, and the Department of Information and Communication Engineering, College of Science and Technology, Basrah University, Basrah, Iraq. He is currently a Professor in electromagnetic and radiofrequency engineering with the University of Bradford, U.K. He is also the Leader of radiofrequency, propagation, sensor design, and signal processing with the School of Engineering and Informatics, University of Bradford, where he is also leading the Communications Research Group. He is a Chartered Engineer. He has many years of research experience in the areas of radio frequency, signal processing, propagations, antennas, and electromagnetic computational techniques. He is a principal investigator for several funded applications to EPSRCs, Innovate U.K., and British Council, and the leader of several successful knowledge Transfer Programmes, such as with Arris (previously known as Pace plc), Yorkshire Water plc, Harvard Engineering plc, IETG Ltd., Seven Technologies Group, Emkay Ltd., and Two World Ltd. He has also been a co-investigator in several funded research projects, including 1) H2020-MSCA-RISE-2024-2028, total, £1.2 million, UoB share £2204 k; Marie Skłodowska -Curie, Research and Innovation Staff Exchange (RISE), titled ''6G Terahertz Communications for Future Heterogeneous Wireless Network;'' 2) HORIZON-MSCA-2021-SE-01-01, Type of Action: HORIZON-TMA-MSCA-SE 2023-2027: ROBUST: Proposal titled ''Ubiquitous eHealth Solution for Fracture Orthopaedic Rehabilitation;'' 3) Horizon 2020 Research and Innovation Programme; 4) H2020 MARIE Skłodowska-CURIE ACTIONS: Innovative Training Networks Secure Network Coding for Next Generation Mobile Small Cells 5G-US; 5) European Space Agency: Satellite Network of Experts V, Work Item 2.6: Frequency selectivity in phase-only beamformed user terminal direct radiating arrays; 6) Nonlinear and demodulation mechanisms in biological tissue (Department of Health, Mobile Telecommunications and Health Research Programme; and 7) Assessment of the Potential Direct Effects of Cellular Phones on the Nervous System (EU: collaboration with six other major research organizations across Europe). He has published more than 800 academic journals and conference papers; in addition, he has coauthored seven books and several book chapters including seven patents. His research interests include computational methods and optimizations, wireless and mobile communications, sensor design, EMC, beam steering antennas, energy-efficient PAs, and RF predistorter design applications. He is a fellow of the Institution of Engineering and Technology and the Higher Education Academy. He was a recipient of the Business Innovation Award for the successful KTP with Pace and Datong companies on the design and implementation of MIMO sensor systems and antenna array design for service localizations. He is the chair of several successful workshops on energy-efficient and reconfigurable transceivers: approach toward energy conservation and CO_2 reduction that addresses the biggest challenges for future wireless systems. He has been the General Chair of the IMDC-IST International Conference, since 2020; a Co-Editor of *Electronics* (MDPI), since 2019; and a Guest Editor of *IET Science, Measurements and Technology* journal, since 2009.